Transmission Coefficient, Resonant Tunneling Lifetime and Traversal Time in Multibarrier Semiconductor Heterostructure

Jyotirmayee Nanda[1], P. K. Mahapatra[2] and C. L. Roy[3]

[1]Department of Physics, National Institute of Technology, Rourkela, India, 769008, email: jnanda_b9@rediffmail.com

[2]Department of Physics and Technophysics, Vidyasagar University, Midnapore, India, 721102, email: pkmahapatra@vidyasagar.ac.in

[3]Department of Physics and Meterology, Indian Institute of Technology, Kharagpur, India 721302

Subject Classification: 73.40

Keywords: Multibarrier resonant tunneling, transmission coefficient, tunneling lifetime, group velocity, traversal time, surface state

Abstract

A computational model based on non-relativistic approach is proposed for the determination of transmission coefficient, resonant tunneling energies, group velocity, resonant tunneling lifetime and traversal time in multibarrier systems ($GaAs/Al_y Ga_{1-y} As$) for the entire energy range $\varepsilon < V_0$, $\varepsilon = V_0$ and $\varepsilon > V_0$, V_0 being the potential barrier height. The resonant energy states were found to group into allowed tunneling bands separated by forbidden gaps. The tunneling lifetime and the traversal time are found to have minimum values at the middle of each allowed band. Further, It is observed that the electrons with energies in the higher tunneling band could tunnel out faster than those with energies in the lower band. Moreover, an additional resonant peak in resonant energy spectrum indicated the presence of a surface state where resonant tunneling occur.

1.Introduction

The resonant tunneling of an electron wave through multiple potential barriers is one of the basic phenomena in quantum mechanics. In a multibarrier system (MBS), the transmission coefficient is the relative probability of an incident electron crossing the multiple barriers. Resonant tunneling in the MBS corresponds to unit transmission coefficient across the structure. One of the most striking features of the multi-barrier systems is the occurrence of quasi-level resonant tunneling energy states. Incident electrons on the MBS with energies equal to any one of these quasi-level resonant energy states suffer resonant tunneling i.e. electrons incident on the MBS with energies equal to resonant state energies tunnel out without any significant attenuation in their intensity. Resonant tunneling is a consequence of the phase coherence of the electron waves in the quantum wells of the MBS. These quasi-level resonant energy states group themselves into tunneling energy bands separated by forbidden gaps. Each allowed energy band comprises (N-1) number of resonant energy states; N being the number of barriers in the MBS.

Research activities on multibarrier resonant tunneling has gained momentum on both theoretical and experimental front since the pioneering work of Tsu and Esaki [1] and Chang et al [2]. This motivation may be attributed to the potential and extensive applications of the resonant tunneling phenomenon in high speed electronic devices that encompasses lasers, modulators, photodetectors and signal processing

devices [1]. The interest in this field has been catapulted to a new height with the advent of epitaxial growth techniques, particularly, the technique of molecular-beam epitaxy (MBE) and metalorganic chemical vapour deposition (MOCVD), through which fabrication of perfect superlattices and multi-quantum-well structures became a reality. Besides, the study of tunneling through MBS provides a deeper understanding of the transport phenomena through semiconductor superlattices and similar structures, such as quantum-dot arrays. Hence, it is plausible to devise theoretical model for resonant tunneling of electrons in such multibarrier structures [3-5] that might help the experimentalists to fabricate ultrahigh-speed electronic and optoelectronic devices. An understanding of the time dependent aspects of tunneling is clearly required for the construction of a kinetic theory for such systems. The simple question of tunneling time seems to be a natural beginning.

Recently, the electronic conductance in double quantum well systems have been reviewed in [5] and the study of tunneling of a particle or a photonic wave packet through an arbitrary number of finite rectangular opaque barriers has also been reported [6]. Analysis on tunneling across an arbitrary shape of potential barrier and the calculation of tunneling coefficients based on the analytic transfer-matrix technique is provided in a general framework by Zhang et al [7]. A deeper insight of the transport phenomena through semiconductor superlattices, resulting from the study of tunneling through multibarrier system, is given in [8].

Crystalline semiconductor superlattices are usually constructed by growing two compounds, such as GaAs/$Al_y Ga_{1-y}$As, where the lattice constants are almost identical. It has been reported by Esaki [9] that the model on superlattices is analogous to the Kronig-Penny model with the following conditions; (i) the barrier

height is the energy mismatch in the conduction band edges of two materials with different compositions, (ii) The masses in the well and barrier regions are different and they correspond to the effective masses at the conduction band edges respectively. Some studies has been reported on the theory of resonant tunneling in superlattices for incident energies less than the height of the potential barrier [10,11]. Experimental evidence has also been found for screening effects from surface states in GaAs/AlGaAs based nanostructures [12].

The resonant quasi-level lifetime, which is referred here after as resonant tunneling lifetime (RTL), is one of the key issues concerning the development of the novel electronic devices based on tunneling. Specifically, determination of the RTL is vital to estimate the frequency limit of high speed tunneling devices. The RTL, τ, in double barrier system has been studied [13-16] and, recently, some effort has been directed to investigate the lifetime in multibarrier systems [17,18]. A striking feature of RTL in the multibarrier systems with more than two barriers is the occurrence of special minima in the resonant lifetime for quasi-level resonant energies in the middle of the allowed tunneling energy bands of the MBS. In [18], the dependences of RTL on the mole fraction of barrier layer(y), well width, and barrier width of GaAs/$Al_y Ga_{1-y}$As superlattices have been explored. It is observed that the tunneling phenomenon is not only characterized by a tunneling rate($1/\tau$) but also by a quantity called the traversal time (τ_R) [19]. The group velocity of the electrons corresponding to the resonant energy states obtained from the ε-k relation in the resonant tunneling energy bands can be used to calculate the traversal time of the electron across the multibarrier structure

for the corresponding incident energy. The traversal time defined in the present context is the time taken by the maxima of a wave packet to cross the multibarrier system. As such to optimize the performance of these quantum tunneling devices, an accurate knowledge of their quasi-levels and the corresponding lifetimes and traversal times are necessary. The estimation of traversal (or transit) time of electrons in a resonant tunneling structure is a stepping stone to model the fast switching of the resonant tunneling devices. Several authors [19-21], over a period of time, have attempted the computation of the traversal time by employing various methods.

By and large, the study of RTL has been confined to the double barrier systems. The reported works in MBS have only discussed the resonant tunneling for electrons with incident energies ε in the range $\varepsilon \langle V_0$, V_0 being the height of the potential barrier. A study of resonant tunneling with incident energies $\varepsilon \geq V_0$ is expected to exhibit the features of the resonant tunneling energy bands more clearly. There is hardly any such attempt to deal with resonant tunneling with incident energies $\varepsilon \geq V_0$ and study theoretically relations of resonant energies and RTL on these factors. Further, the resonant tunneling energies, RTL, and the transition time depend on the parameters such as the height of the potential barrier controlled through the mole fraction of barrier material vis-a-vis the well material, the thickness of the barrier and well layers and the number of barriers in the structure. As far as the authors' knowledge goes, there is hardly any report on the computation of the traversal time in the multibarrier systems.

In view of the above, in this paper, we have focussed our research work on the study of the resonant tunneling time with incident energies both for $\varepsilon < V_0$ and $\varepsilon \geq V_0$ and the study of traversal time for multibarrier systems. Here we employ the non-relativistic approach to develop necessary expressions governing the transmission coefficient of electrons tunneled through the multibarrier heterostructure (GaAs/$Al_y Ga_{1-y}$ As). However, the results presented in this paper correspond to a specific structure with y=0.3 in the above composition. The derivation of the transmission coefficient is based on the transfer matrix approach. The effect of number of barriers, number of cells in the well region, and the barrier region on the resonant energy states is also investigated. The lifetime, group velocity, and the traversal time of electron are computed for the above multibarrier system. Computation of resonant tunneling lifetime requires the evaluation of the half-width at half-maximum of the resonant peaks around the resonance energies ε_m. The half maximum value of the ε_m is obtained from the graph of tunneling coefficient versus incident energy by employing a search technique. The group velocity is computed by interpolating the dispersion curve (ε versus k) followed by computing the derivative at the interpolated points.

Section 2 deals with derivation of the transmission coefficient and formulae used for the determination of lifetime, group velocity and traversal time. The parameters used in our simulation are presented in Section 3. The effects of the number of barriers, number of cells in the well region and barrier region on the resonant energy are presented in Section 4.2. Studies on resonant tunneling lifetime, group velocity, and traversal time are dealt in Sections 4.3 and 4.4. The concluding remarks are presented

in Section 5. **The algorithm for the search program for finding the resonant tunneling energies,the width of resonant peaks and the resonant life time are given in the appendix.**

2. Non-relativistic treatment of tunneling through symmetric multibarrier semiconductor heterostructure

The tunneling of electrons through multibarrier semiconducting heterostructures can be better understood by a model, as shown in Fig. 1(a). In this model, the multibarrier structure is obtained by alternately stacking layers of semiconducting materials, namely, GaAs and $Al_y Ga_{1-y} As$. These two materials have similar band structures but different energy gaps. The schematic energy diagram for the stacking layers is shown in Fig. 1(b). The small gap material GaAs forms the well while the large gap material $Al_yGa_{1-y}As$ forms the barrier of the superlattice. The barrier height is assumed [22] to be 88% of the difference between the band gaps of two materials. The MBS with well and barrier regions, originated from the band offset is shown in Fig.1(c). The model consists of N barriers of thickness **'**b', and N-1 wells of thickness 'a'. Thus, the superlattice has a period 'c', where c = (a + b). The height of the potential barrier is considered as V_0.

2.1. Transmission coefficient

To deal with the problem one need to consider the one-dimensional time independent Schrödinger equation**, specifically the BenDaniel-Duke equation [23]** for the electron in the potential V(x) which appears as:

$$\left[-\frac{\hbar^2}{2}\frac{d}{dx}\frac{1}{m^*}\frac{d}{dx}+V(x)\right]\psi(x)=\varepsilon\psi(x) \qquad (1)$$

Where,

m^* **is the position dependent effective mass and have different values for the well and the barrier material,**

$$V(x)=\begin{cases} V_0 & for \quad nc-b/2 \le x \le nc+b/2 \\ 0 & otherwise \end{cases} \tag{2}$$

The wave functions of the time independent Schrodinger equation in the nth well region has the form:

$$\psi_n^{(w)}(x) = A_{2n-1}\, e^{ik_1 x} + B_{2n-1}\, e^{-ik_1 x} \tag{3}$$

where, $k_1^2 = 2m_w^*\varepsilon/\hbar^2$, $n = 1,2,\cdots N$, and N is the number of barriers.

The wave function in the barrier region can be obtained as

$$\psi_n^{(b)}(x) = \begin{cases} A_{2n}\, e^{-k_2 x} + B_{2n}\, e^{k_2 x} & for\ \varepsilon \langle V_0 \\ A_{2n} + B_{2n}\, x & for\ \varepsilon = V_0 \\ A_{2n}\, e^{ik_3 x} + B_{2n}\, e^{-ik_3 x} & for\ \varepsilon \rangle V_0 \end{cases} \tag{4}$$

where, $k_2^2 = 2m_b^*(V_0-\varepsilon)/\hbar^2$ *and*
$k_3^2 = 2m_b^*(\varepsilon - V_0)/\hbar^2$

The following effective mass dependent boundary conditions are used at the interfaces of the nth barrier with nth and (n+1)th well region which conserves the probability

$$\begin{aligned} &\psi_n^{(w)}(x)\Big|_{nc-b/2} = \psi_n^{(b)}(x)\Big|_{nc-b/2} \\ &\frac{1}{m_w^*}\frac{d\psi_n^{(w)}}{dx}\bigg|_{nc-b/2} = \frac{1}{m_b^*}\frac{d\psi_n^{(b)}}{dx}\bigg|_{nc-b/2} \end{aligned} \tag{5}$$

$$\psi_n^{(b)}(x)\,|_{nc+b/2} = \psi_{n+1}^{(w)}(x)\,|_{nc+b/2} \tag{6}$$

$$\frac{1}{m_b^*}\frac{d\psi_n^{(b)}}{dx}\bigg|_{nc+b/2} = \frac{1}{m_w^*}\frac{d\psi_{n+1}^{(w)}}{dx}\bigg|_{nc+b/2}$$

Where, m_b^* and m_w^* are the effective masses in the barrier and well region respectively.

The coefficients of the electron wave across the first potential barrier are related as:

$$\begin{bmatrix} A_3 \\ B_3 \end{bmatrix} = M_1 \begin{bmatrix} A_1 \\ B_1 \end{bmatrix} \tag{7}$$

Where M_1 is a (2×2) matrix, called as transfer matrix.

With the help of boundary conditions Eqs.(5)-(6), we obtain the elements of M_1 as given below.

$$(M_1)_{11} = (M_1)_{22}^* = \begin{cases} \left(\cosh k_2 b + \dfrac{k_2^2 f^2 - k_1^2}{2ik_1k_2f}\sinh k_2 b\right)e^{-ik_1 b} & for\ \varepsilon \langle V_0 \\ \left(1 - \dfrac{k_1 b}{2if}\right)e^{-ik_1 b} & for\ \varepsilon = V_0 \\ \left(\cos k_3 b - \dfrac{k_3^2 f^2 + k_1^2}{2ik_3k_1f}\sin k_3 b\right)e^{-ik_1 b} & for\ \varepsilon \rangle V_0 \end{cases} \tag{8}$$

$$(M_1)_{12} = (M_1)^*_{21} = \begin{cases} \dfrac{k_1^2 + k_2^2 f^2}{2ik_1k_2f}\sinh k_2 b & for \varepsilon < V_0 \\ \dfrac{k_1 b}{2if} & for \quad \varepsilon = V_0 \\ \dfrac{k_1^2 - k_3^2 f^2}{2ik_1k_3f}\sin k_3 b & for \quad \varepsilon > V_0 \end{cases} \tag{9}$$

$f = m_w^* / m_b^*$

And det M_1=1.

Now, let us generalize the problem to multiple potential barriers. The (2×2) matrix M_n , which relates the coefficient matrix $\begin{bmatrix} A_{2n-1} \\ B_{2n-1} \end{bmatrix}$ of the wave on the left of nth barrier to that on the right of the barrier $\begin{bmatrix} A_{2n+1} \\ B_{2n+1} \end{bmatrix}$ appears as :

$$M_n = (F^*)^{n-1} M_1 F^{n-1} \tag{10}$$

where, $F = \begin{bmatrix} e^{ikc} & 0 \\ 0 & e^{-ikc} \end{bmatrix}$ and $n = 1,2\cdots N.$

Thus, the transfer matrix W_N which relates the coefficient matrix of the incoming and outgoing wave in the N barrier system can be expressed as:

$$\begin{bmatrix} A_{2N+1} \\ B_{2N+1} \end{bmatrix} = [W_N] \begin{bmatrix} A_1 \\ B_1 \end{bmatrix} \tag{11}$$

where,

$$W_N = M_N M_{N-1} \cdots\cdots\cdots M_2 M_1 \tag{12}$$

Substituting M_n from Eq. (10) in Eq. (12), the transfer matrix takes the form

$$W_N = (F^*)^N G^N \tag{13}$$

where, the matrix $G = M_1 F$ (14)

The matrix W_N is Hermitian and its determinant has unit value.

G matrix can be diagonalized to the matrix G_d as $S^{-1} G S = G_d$; S being the diagonalizing matrix of the matrix G and $G_d = \begin{bmatrix} \lambda_1 & 0 \\ 0 & \lambda_2 \end{bmatrix}$; λ_1 and λ_2 ,being the eigenvalues of the matrix G, satisfy the following relations.

$$\lambda_{1,2} = \frac{G_{Tr} \pm \sqrt{G_{Tr}^2 - 4}}{2}$$

where G_{Tr} is the trace of matrix G.

$$G_{T\gamma} = \begin{cases} 2\left[\cos k_1 a \cosh k_2 b + \dfrac{k_2^2 f^2 - k_1^2}{2k_1 k_2 f} \sin k_1 a \sinh k_2 b\right] & for\ \varepsilon < V_0 \\ 2\left[\cos k_1 a - \dfrac{k_1 b}{2f} \sin ka\right] & for\ \varepsilon = V_0 \\ 2\left[\cos k_1 a \cos k_3 b - \dfrac{k_3^2 f^2 + k_1^2}{2k_1 k_3 f} \sin k_1 a \sin k_3 b\right] & for\ \varepsilon > V_0 \end{cases} \tag{15}$$

Here, $\lambda_1 + \lambda_2 = G_{Tr}$ and $\lambda_1 \lambda_2 = 1$. So that,

$$\begin{aligned} \lambda_1 = \frac{1}{\lambda_2} = e^{i\theta} \qquad & \theta = \cos^{-1}\left(G_{tr}/2\right) \qquad for \quad G_{Tr} \langle 2 \\ \lambda_1 = \lambda_2 = 1 \qquad & for \quad G_{Tr} = 2 \\ \lambda_1 = \frac{1}{\lambda_2} = e^{\theta} \qquad & \theta = \cosh^{-1}\left(G_{tr}/2\right) \qquad for \quad G_{Tr} \rangle 2 \end{aligned} \tag{16}$$

Using these relations, the transfer matrix W_N can be written as

$$W_N = \left(F^*\right)^N S\, G_d^N\, S^{-1} \ . \tag{17}$$

The Transmission coefficient T_N across N barriers can be obtained as

$$T_N = \frac{\left|A_{2N+1}\right|^2}{\left|A_1\right|^2} \tag{18}$$

As there is no reflected electron beyond the right end of the multibarrier system, one can set $B_{2N+1} = 0$. Using this fact together with the Eqs.(11) and(18) T_N can be obtained as

$$T_N = \frac{1}{\left|(W_N)_{11}\right|^2} = \frac{1}{1+\left|(W_N)_{12}\right|^2} \tag{19}$$

$(W_N)_{12}$ can be obtained from Eq. (17) as:

$$(W_N)_{12} = e^{-ik_1Nc} G_{12} \frac{\lambda_2^N - \lambda_1^N}{\lambda_2 - \lambda_1} \tag{20}$$

Substituting Eqs. (14) and(16) on Eq. (20), $(W_N)_{12}$ appears as

$$\left|(W_N)_{12}\right|^2 = \begin{cases} \left|(M_1)_{12}\right|^2 \left|\dfrac{\sin N\theta}{\sin\theta}\right|^2 & for \quad G_{Tr} < 2 \\ \left|(M_1)_{12}\right|^2 N^2 & for \quad G_{Tr} = 2 \\ \left|(M_1)_{12}\right|^2 \left|\dfrac{\sinh N\theta}{\sinh\theta}\right|^2 & for \quad G_{Tr} > 2 \end{cases} \tag{21}$$

The transmission coefficient T_N across the N barrier system for the three different situations corresponding to the incident energy $\varepsilon < V_0$, $\varepsilon = V_0$ and $\varepsilon > V_0$ can be obtained from the Eq.(19) in combination with Eqs.(21) and (9).

2.2. Resonant Tunneling Energies

The resonant tunneling across the N barrier system corresponds to the condition $T_N = 1$. The incident energies of the electron, for which the resonant tunneling condition is satisfied, is termed as resonant tunneling energies. Here we have found the resonant tunneling energies in the multibarrier system from the T_N vs ε curve by a computer program using a search technique. However it would

be worthwhile to highlight some of the salient features of the resonant tunneling energy states.

(a) Eq. (16) in combination with Eq. (15) is akin to the energy relation for a lattice of period (a+b) calculated using effective mass dependent Kronig-Penny model. The allowed energy bands are restricted to values of $G_{Tr} < 2$ which corresponds to the allowed values of $\cos\theta$ in Eq.(16). Hence the resonant tunneling states group themselves to allowed tunneling energy bands separated by forbidden gaps.

(b) As can be seen from Eq. (19) in combination with Eq. (21), the resonant state will correspond to $SinN\theta = 0$ where θ is given in Eq. (16). Thus, there occurs N-1 values of resonant energies in each band for $\theta = n\pi / N, \quad n = 1, 2, ..., N-1.$ These values of θ correspond to the wave vectors $n\pi/L$ in a superlattice of length $L = Nc$. Thus for the N-barrier superlattice with $(N-1)$ wells, each allowed mini energy band will contain (N–1) number of resonance energy states corresponding to the $(N-1)$ values of the wave vector.

(c) During the resonance tunneling, the electron energy resonates at the bound states of quantum well. Hence, the number of allowed bands in these multibarrier systems is found to be equal to the number of bound energy states in the single finite quantum well having the same parameters as that of the MBS. It may be worth noting here that the number of bound states, j, for $\varepsilon < V_0$ in a finite well depends on the width, a, and potential height, V_0, of the quantum well through the relation :

$$j = Int(\beta) + 1 \tag{22}$$

Where, $\beta = \sqrt{\left(\frac{a}{\pi}\right)^2 \left(k_1^2 + k_2^2\right)_{E=V}} = \sqrt{\frac{8a^2 m_1^* V}{h^2}}$

and Int (β)=Integer value of β

Hence due to phase coherence the number of tunneling bands in multibarrier systems for $\varepsilon<V_0$ will be equal to 'j' which depends on the well width and the height of the potential barrier and is independent of the barrier width.

2.3. Resonant Tunneling Lifetime

The RTL is computed using the energy uncertainty condition at energy corresponding to resonant tunneling and the formulae [10] is given below.

$$\tau = \frac{\hbar}{2\Delta\varepsilon_m} \tag{23}$$

Where τ is the RTL, $\hbar = \frac{h}{2\pi}$, h is the Planck's constant and $\Delta\varepsilon_m$ is the half-width of the resonant peak at half-maximum of the resonant peak around the resonance energy ε_m. The halfwidth $\Delta\varepsilon_m$ is obtained from the graph of tunneling coefficient versus incident energy by computational methods. Specifically, our computational method employs a search technique to determine the values of the half-maximum of the resonant peak.

2.4. Traversal Time

The traversal time of electrons for energies corresponding to resonant tunneling is defined by [19]

$$\tau_R = \frac{L}{v_g} \tag{24}$$

Where L is the total length traversed by the electron and v_g is the group velocity defiened through the relation $v_g = \frac{1}{\hbar}\frac{d\varepsilon}{dk}$. k is the wavevector defined as $\frac{n\pi}{L}$, where $n = 1,2,\cdots\cdots\cdots(N-1)$. The group velocity v_g is obtained in two steps: (i) First, the points of the ε versus k curve are interpolated by Lagrangian interpolation technique, (ii) In the second step, the derivative at the necessary points are computed.

3.Numerical Analyses:

The numerical analyses is basically concerned with the computation of (i) the transmission coefficient across multibarrier systems for incident energies $\varepsilon < V_0$, $\varepsilon = V_0$ and $\varepsilon > V_0$,(ii) resonant tunneling energies for which the transmission coefficient is unity,(iii)the resonant tunneling lifetime and (iv) the group velocity and traversal time across the barrier. The procedure for computing the transmission coefficient in the non-relativistic treatment is based on numerical computation of Eq.(19) in combination with Eqs.(21) and (9). Thereafter these data points are sorted to obtain the resonant tunneling energies for which transmission coefficient is unity. The half-width at half maximum, $\Delta\varepsilon_m$, around each resonant tunneling energies are obtained by first finding the energies for which T_N is minimum on both the left and the right side of the resonant tunneling peak using a search program and then finding the energies $\varepsilon_{L_{1/2}}$ and $\varepsilon_{R_{1/2}}$ on both the sides of the peak where $T_N = (T_{max}+T_{min})/2$; T_{max} being the transmission

coefficient at the resonant peak and T_{min} correspond to the minimum transmission coefficient on the corresponding side of the resonant peak. **The algorithm of the search program used is given in the appendix**. The half width $\Delta\varepsilon_m$ around each peak is obtained from the relation $\Delta\varepsilon_m = \varepsilon_{R_{1/2}} - \varepsilon_{L_{1/2}}$ The resonant tunneling life time for each resonant energy is then calculated from Eq.(23) The traversal time is calculated for each energy state by finding out the group velocity associated with the resonant states in each resonant tunneling band by using Lagrangian interpolation technique and then we use the principle that traversal time corresponding to a resonant state is equal to the ratio of the length of the multibarrier system and the group velocity associated with the corresponding resonant state. In order to bring forth the variation of the tunneling and traversal times in the multibarrier systems , the problem is studied for various values of barrier width, well width and the number of barriers in the MBS. For the numerical evaluation of T_N, ε_m, τ and τ_R, we have chosen the GaAs/$Al_yGa_{1-y}As$ (y =0.3) superlattice with the values of various parameters as follows:

a = the well width = ncw x a_w, where ncw is the number of cells in the well material in each well slab and a_w is the lattice constant of the well material GaAs.

a_w = 5.6533 Å

b= the barrier width = ncb x a_b, where ncb is the number of unit cells of the barrier material in each barrier slab and a_b is the lattice constant of the barrier material $Al_{0.3}Ga_{0.7}As$.

$a_b = 5.65564$ Å.

m_w^* and m_b^* = the effective masses of the well (GaAs)and the barrier ($Al_{0.3}Ga_{0.7}As$) region materials of the superlattice

= 0.065 m_0 and (0.067 + 0.083x 0.3) m_0 ; m_0 is the free electron mass.

E_{g1} and E_{g2} = energy band gap in the well and barrier materials

= 1.428 eV and (1.424 + 1.247x *0.3*) eV.

V = height of the potential barrier = 0.88 ($E_{g2} - E_{g1}$)

The energy band gap of $Al_yGa_{1-y}As$ becomes indirect when the value of mole fraction (y) exceeds 0.45, and hence does not conform to the band diagram (shown in Fig. 1(b)). Therefore, for the present calculations we have considered y=0.3.

4. Results and Discussion

4.1 Transmission coefficient:

The transmission coefficient for GaAs/ $Al_{0.3}Ga_{0.7}As$ multibarrier systems is calculated on the basis of Eq.(19) in combination with Eqs.(21)and (9). Fig(2) depicts the transmission coefficient versus incident energy. The graphs 2(a) and 2(b) show the variation of T_N versus ε for systems with ncw=5, ncb=5 having 3 barriers and 9 barriers respectively. The T_N versus ε curve for 9 barrier systems with ncw=5, ncb=4 is presented in graph 2(c) and that for ncw=8 and ncb=5 in graph 2(d). The graphs clearly show that the transmission coefficient varies rapidly and attains the value of unity for certain incident energies. These energies are referred as resonant energies both for $\varepsilon < V_0$ and $\varepsilon > V_0$. These resonant energies group themselves into

allowed tunneling bands separated by forbidden gaps. In the forbidden region the transmission coefficient remains zero. In each allowed tunneling band there are N-1 number of resonant states; N being the number of barriers in the system. In the first band the variation of T_N seems to be rapid and becomes zero in the neighbourhood of the maxima. However, the variation of T_N is not that rapid for resonant energies in the higher bands. The T_N in the higher bands remains near the maximum value of unity and the peaks are less sharp.

4.2 Resonance Energies

The resonant energies corresponds to the condition T_N =1 and are obtained from the T_N versus ε graphs by using the search technique. Fig. 3 display the resonant energies for systems with varied ncw, ncb and N. As has been mentioned these resonant states are for allowed tunneling bands separated by forbidden bands both for $\varepsilon < V_0$ and $\varepsilon > V_0$ with each allowed band containing N-1 resonant states. However, there is one extra energy state observed in each system where T_N become one. We feel this might be a surface state. **To find the origin of this extra resonant energy state, we checked the transmission coefficient for the N-1 values of energies corresponding to** $\theta = n\pi / N, \quad n = 1, 2, ..., N-1.$ **in each band directly from Eq(19)-(21) using a different method. It is worth pointing here that these values of** θ **correspond to the allowed k values of a band as explained in (b) of subsection2.2. It is found that the resonant energies obtained through search technique tallies with those obtained through the second method for the band states. It is thus confirmed that the extra resonant state is certainly not a band state and can be accounted only as a surface state arising due to the finiteness of**

the system[24-25] and termination of the periodic potential. The surface states are indicated in the figures by an arrow mark.

Fig. 3(a) presents the resonant energy states for ncw=5 and ncb=5 but for the number of barriers N to be 5, 7, 9. We have considered incident energies up to 1.5eV. In all these three cases we have obtained three allowed tunneling bands with each allowed band containing N-1 resonant states. For low values of N, ε_m lies in the center of the band, as N increases ε_m spreads out from the central regions of the bands towards the edges. From this figure it can be clearly seen that the position of the surface state remains independent of the number of barriers. Fig. 3(b) depicts the resonant energy state for 9 barrier system with constant barrier width with ncb=5 and varying well width with ncw=2 ,5,8 respectively. The number of allowed tunneling bands increases form 2 to 4 when we move from ncw=2 to ncw=8. This observation is in conformity with the number of allowed bands given in Eq.(22). Further, with increase in ncw, the width of the allowed bands and the forbidden gaps becomes narrower. The energies of the bound state of the quantum wells move to lower energy values as the width of the well increases. It is worth pointing that in an infinite quantum well the energies of the bound states are inversely proportional to the square of the well width and any increase in well width will cause the bound states to shift to the lower values. Here, the surface states have the same values for all the three cases of well width suggesting that the energy of the surface state is independent of the well width only when the barrier width remains constant. Fg. 3(c) represents the resonant tunneling energies for the 9 barrier system for constant well width i.e. ncw=5 and varying barrier width ncb=4,5,6. An increase in barrier width causes a

decrease in the overlap interactions between the states of adjacent wells resulting in a decrease in the bandwidth which is evident in the graph Fig. 3(c) as we go from ncb=4 to ncb=6. Moreover, the surface state moves towards the lower energy state with an increase in ncb. In Fig. 3(d), resonant energies are presented for a system for 9 barrier system having total number of cells constant while varying ncw and ncb simultaneously. With various combination of ncw and ncb, it is observed that the surface state gradually moves towards the higher energy state.

4.3 Resonant Tunneling Lifetime

Tunneling lifetime values are calculated using Eq. (23). Fig. 4 shows the variation of RTL(τ), for the system with ncw=5, ncb=5 while the number of barriers varied from 5 to 9. The following significant features can be noticed.

(a) The profile of τ, for the smallest/largest value of ε_m in all allowed energy bands, show similar characteristic irrespective of the number of barriers.

(b) The τ values for the resonant states decrease as we move towards higher tunneling bands. This is due to the fact that the electrons in resonant states in the higher bands can tunnel faster than those in lower bands owing to their higher energy.

(c) The lifetime for the resonant state at the near middle of the band show a minimum. This observation corroborates the phenomenon observed by Arif et al [17] in GaAs/$Al_y Ga_{1-y}$As superlattices. This **minimum value of the lifetime** implies that the electron in the middle of the band tunnel out faster than those with other values of ε_m in the same band. Moreover, an increase in N in a system accompanies an increase in τ for the same values of ε_m.

(d) The intraband variation of τ with ε_m decreases as we go towards the higher bands. Apparently, τ seems to decrease in the second band with the increase in energy of the resonant state.

(e) In the third band, there is slight variation in the τ values observed for a particular N. Hence, we can say that there is little variation in the tunneling rate.

4.4. Group velocity and traversal time

The dispersion curves are plotted for multibarrier systems having ncw =5, ncb=5 and N=5,7 and 9 respectively. Using Langragian interpolation data points are interpolated. Thereafter, the group velocity of the electrons is computed. The group velocity 'v_g' obtained after Langragian interpolation for various N values are shown in Fig. 8. In this figure the v_g for only the first two allowed bands are shown. In the first allowed band v_g is found to be highest in the middle of the band. The v_g values gradually increase with the increase in ε_m values in the second allowed band. Moreover, the v_g values slightly increase when N is increased from 5 to 9.

The traversal time computation is performed by using Eq. (24). The total length traversed by electron is calculated using the relation, $L = ncw \times a_w \times (N-1) + ncb \times a_b \times N$. The traversal time '$\tau_R$' corresponding to resonant energies are plotted in Fig. 6, only for first two allowed bands. The profiles of τ_R show the same trend as it is observed in the plots for lifetime and have values of the same order as τ. **The occurrence of minimum of τ_R at values of ε_m around the middle of an allowed band can be explained using the fact that the group**

velocity of an electron is the highest at the middle of an allowed band. Consequently, an electron with ε_m in the middle of any allowed band will tunnel out faster than those with other values of ε_m in the same band.

5. Conclusions

In this work, a model for computation of transmission coefficient for multibarrier semiconductor heterostructure is proposed. The resonant energy values are found to be dependent on the number of barriers, number of cells in the well region and number of cells in the barrier region. The resonant energy states group themselves into allowed tunneling bands separated by forbidden gaps for energies $\varepsilon < V_0$, as well as $\varepsilon > V_0$, each tunneling band containing (N-1) number of states in a N barrier system. The results indicate the presence of a new surface state in the resonant energy spectrum. The order of RTL values are found to be in good agreement with the previously reported values for the same type of superlattices. The lifetime and the traversal time for the resonant states at the near middle of each band show a minimum. The resonant tunneling life time and the traversal time are found to have almost similar values. **It is worth pointing that the traversal time defined by Eq(24) at the resonant energies for which $k = \frac{n\pi}{L}$ will reduce to a form similar to that of the resonant life time given through Eq.(23).** The resonant tunneling lifetime, group velocity, and the traversal time presented in this work will be useful in understanding the physical mechanisms of the resonant tunneling phenomena in the multibarrier systems and help in developing appropriate resonant tunneling devices. We also expect the work to initiate a more rigorous study of the surface state in the tunneling energy band in the multibarrier systems.

APPENDIX

Algorithm of the search program to locate the maxima, minima, and the half-widths of the resonant transmission peaks and to compute resonant lifetime.

Step 1: The transmission coefficient (T_N) for the multibarrier system is computed for incident energies, ε ,in the range 0-1.5eV with a step length of 0.00001eV, on the basis of Eqs. (19)-(21), after setting the values for the parameters N, n_w. n_b, a_w, a_b and V. The results are stored in a data file as n, E(n) [=0.00001*n eV] and T(n).

Step2: T(1)= 0 and is taken as the minimum to the left of the first transmission maxima. Hence we set nminl=1, Eminl=E(1) and Tminl=T(1) respectively.

Step3: The maxima is searched by an iterative process starting from n=nminl onwards and satisfy the condition $T(n-m) \le T(n) \ge T(n+m) \quad for\ m = 1,2...9$ **and** $T(n-10) < T(n) > T(n+10)$ **The corresponding values are stored as nmax = n, Emax = E(n), and Tmax = T(n) respectively.**

Step4: The left half maximum of the peak is defined as Tmidl=(Tminl+Tmax)/2. The corresponding value of energy at halfmaximum is found by an iteration starting from n=nminl to nmax and for which ABS(Tmidl –T(n))is the smallest. The corresponding values are stored as nmidl = n, Emidl = E(n), and Tmidl=T(n) respectively.

Step5: The minima of the peak on the rightside of maxima is found by an iterative process starting from n=nmax onwards and satisfy the condition $T(n-m) \ge T(n) \le T(n+m) \quad for\ m = 1,2...9$ **and** $T(n-10) > T(n) < T(n+10)$ **The**

corresponding values are stored as nminrl = n, Eminr = E(n), and Tminr=T(n) respectively.

Step6: The right half maximum of the peak is defined as Tmidr=(Tmax+Tminr)/2. The corresponding value of energy at half maximum is found by an iteration starting from n=nmax to nminr and for which ABS(Tmidr –T(n))is the smallest. The corresponding values are stored as nmidr = n, Emidr = E(n), and Tmidr=T(n) respectively.

Step7: The width at half maximum of the resonant peak is equal to the difference (Emidr-Emidl) and the resonant lifetime for the corresponding resomant energy Emax is is computed on the basis of Eq.(23).

Step8: The right minima of the previous peak is the left minima for the succeeding peak. Hence we reset nminl=nminr, Eminl=Eminr, and Tminl=Tminr and Step3 to Step8 are repeated until all the data points are exhausted.

The algorithm does not have any limitations in regard to the parameters like the number of barriers N ,or others as listed in Step1. The only limitations to the search technique will depend on the data handling capability of the software used.

References:

[1] R. Tsu, L. Esaki, Appl. Phys. Lett. 22 (1973) 562.

[2] L. L. Chang, L. Esaki, R. Tsu, Appl. Phys. Lett. 24 (1974) 593.

[3]H. Yamamoto, Y. Kaniemarakwa, K. Taniguchi, Appl. Phys. A 50 (1990) 577.

[4] C. L. Roy, Arif Khan, Phys. Stat. Sol. (b) 176 (1993) 101.

[5] J. E. Hasbun, J. Phys: Condens. Matter 15 (2003) R143-R175.

[6] S. Esposito, I. N. di Fisica, S. di Nipoli, DSF-17, [arxiv- Quanta.ph/0209018v1], 2002.

[7] A. Zhang, Z. Cao, Q. Shen, X. Dau, Y. Chen, J. Phys. A 33 (2000) 5449.

[8] P. J. Bishop, M. E. Daniels, V. K. Ridley, Semicondt. Sci. Technol. 13 (1998) 482.

[9] L. Esaki, IEEE J. QE-22, (1986) 1611.

[10] P. J. Price, Phys. Rev. B 38 (1988) 1994.

[11] K. H. Ploog, "Materials and Devices: III-V Quantum System Research", (Ed.), Chapter 11, 1994.

[12] C. T. Liang, C. G. Smith, M.Y. Simmons, D. A. Ritchie, M. peeper, Physica E, 22 (2004) 570.

[13] C. J. Arsenault, M. Meunier, Phys. Rev. B 39 (1989) 8739.

[14]H. Xu, M. Zhu, B. Hou, Phys. Lett. A 223 (1996) 227.

[15] A. M. Elabsy, Physica B 292 (2000) 233.

[16] H. Z. Xu, Y. Okada, Physica B 305 (2001) 113.

[17] Arif Khan, P. K. Mahapatra, C. L. Roy, Phys. Lett. A 249 (1998) 512.

[18] Arif Khan, P. K. Mahapatra, S. P. Bhattacharya, S. Noor Mohammad, Phil. Mag. 21, (2004) 547.

[19] M. Buttiker, Phys. Rev. B 27 (1983) 6178.

[20] A. F. M. Anwar, A. N. Khondker, M. Rezwan Khan, J. Appl. Phys. 65 (1989) 2761.

[21] M. A. de Moura, D. F. Albuquerque, Sol. Stat. Commun. 74 (1990) 353.

[22] D. Mukherjee, B. R. Nag, Phys. Rev. B 12 (1975) 4338.

[23] BenDaniel D. J. and Duke C. B., Phys. Rev. 152 (1966) 683.

[24] C. L. Roy and P. K. Mahapatra, Phys. Rev. B25 (1982) 1046

[25] M. Steslicka, Progress in surface Science 50 (1995) 65.

Figure Captions

Fig. 1: (a) Schematic diagram of a binary superlattice obtained by alternately stacking layers of semiconducting materials (GaAs and $Al_{0.3}Ga_{0.7}As$). (b) Energy Band diagram of stacking layers. (c) The multibarrier heterostructure with well and barrier regions originating from the band offset.

Fig. 2. Transmission coefficient versus electron energy for GaAs/$Al_{0.3}Ga_{0.7}As$ superlattice by varying number of barriers 'N', number of cells in the well region 'ncw', number of cells in the barrier region 'ncb'. The arrow indicates the position of the surface state**. The star symbol indicates the transmission coefficient for E=V_0.** (a) N=3, ncw=5, ncb=5, (b) N=9, ncw=5, ncb=5, (c) N=9,ncw=5, ncb=4, (d) N=9, ncw=8, ncb=5.

Fig. 3. Resonant energy (E_m) values for GaAs/$Al_{0.3}Ga_{0.7}As$ superlattice. **The arrow indicates the position of the surface state**. (a) the number of barriers 'N' is varied from 5 to 9, and the number cells in the well region ncw=5, the number cells in the barrier ncb=5. (b) N=9, ncw=2,5,8 , and ncb is fixed at 5. (c) N=9, ncw is fixed at 5, and ncb=4,5,6. (d) N=9, both ncw and ncb are varied simultanesously keeping the total no of cells constant.

Fig. 4. Variation of resonant tunneling lifetime (τ) with resonance energies (ε_m) for GaAs/$Al_{0.3}Ga_{0.7}As$ superlattice with different values of number of barriers (N). The number of cells in the well region, ncw=5 and number of cells in the barrier region, ncb=5. The star symbol indicates the surface state.

Fig. 5. Variation of group velocity (v_g) with resonant energies (ε_m) for GaAs/$Al_{0.3}Ga_{0.7}As$ superlattice with different values of number of barriers (N). The

number of cells in the well region, ncw=5 and number of cells in the barrier region, ncb=5. Two allowed energy bands are shown.

Fig. 6. Traversal time (τ_R) versus resonant energies (ε_m) for $GaAs/Al_{0.3}Ga_{0.7}As$ superlattice with different values of number of barriers (N). The number of cells in the well region, ncw=5 and number of cells in the barrier region, ncb=5. Two allowed energy bands are shown.

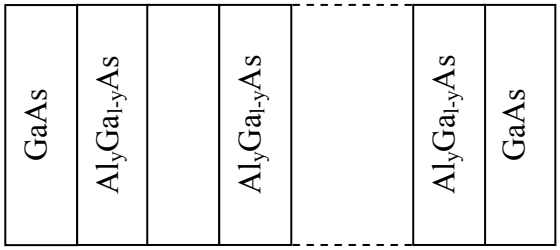
GaAs
$Al_yGa_{1-y}As$
$Al_yGa_{1-y}As$
$Al_yGa_{1-y}As$
GaAs

(a)

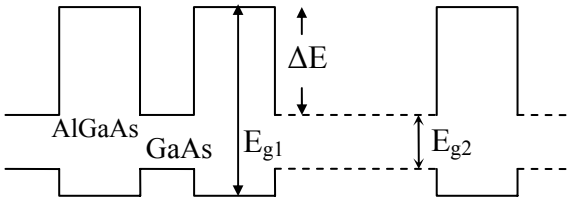
ΔE
AlGaAs
GaAs
E_{g1}
E_{g2}

(b)

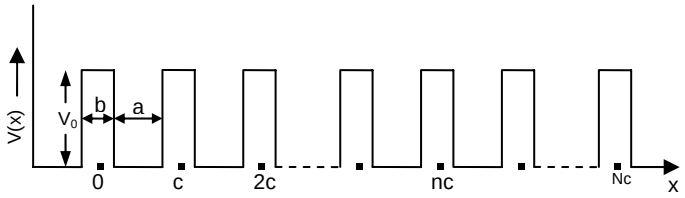
V(x)
V_0
b
a
0
c
2c
nc
Nc
x

(c)

Figure 1

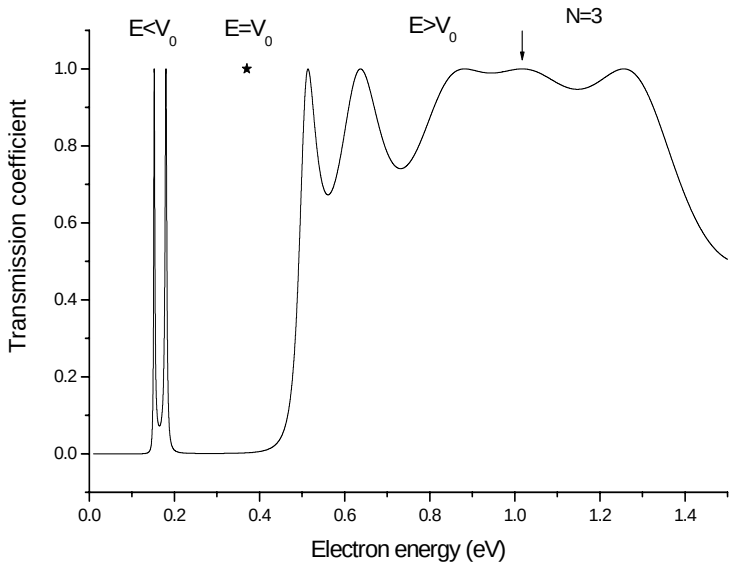

Figure 2(a)

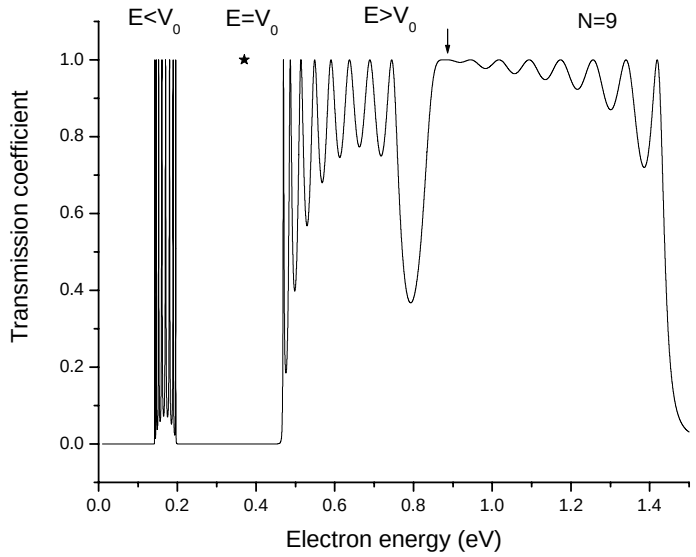

Figure 2(b)

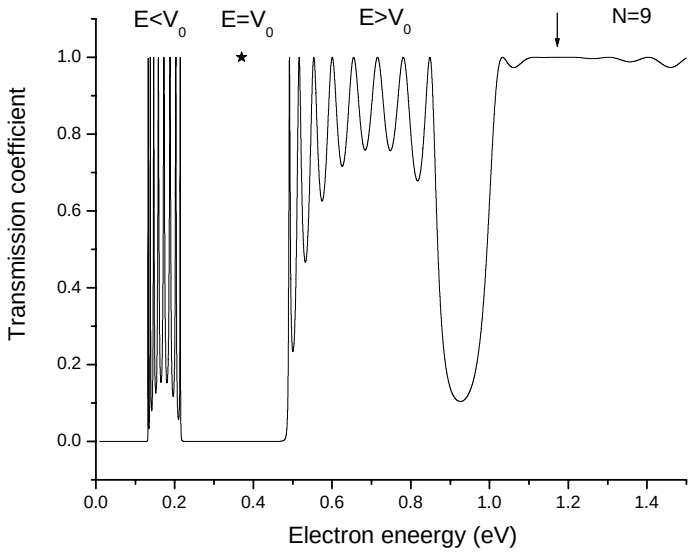

Figure 2(c)

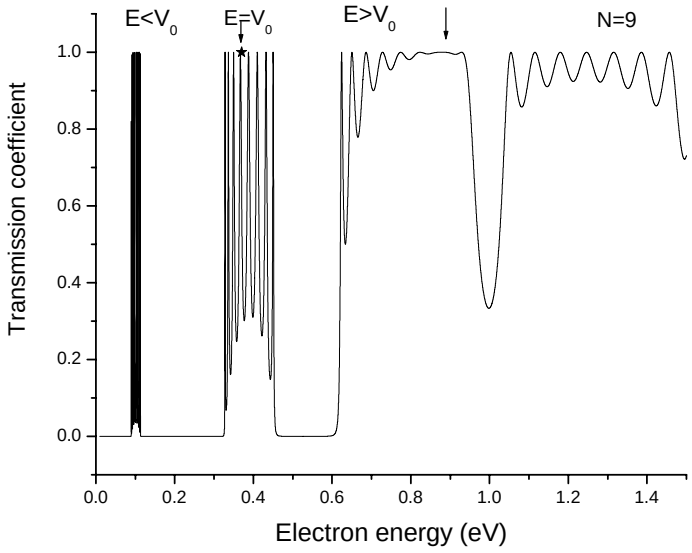

Figure 2(d)

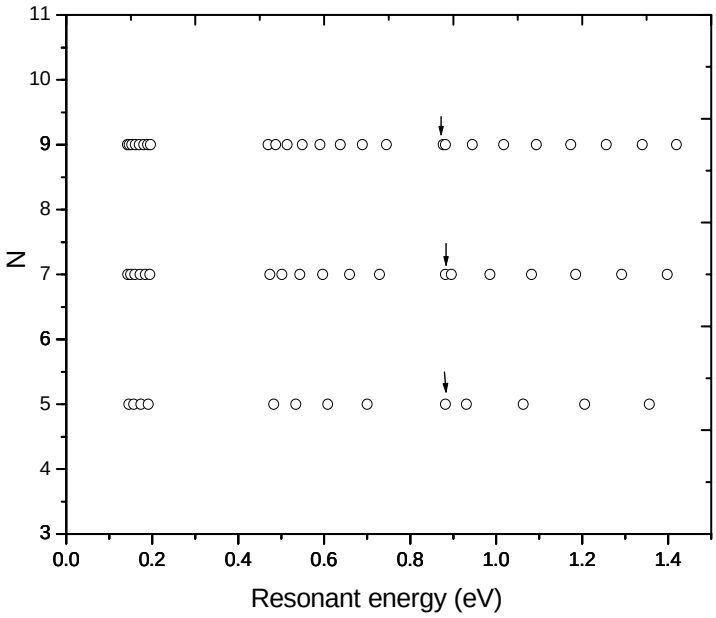

Figure 3(a)

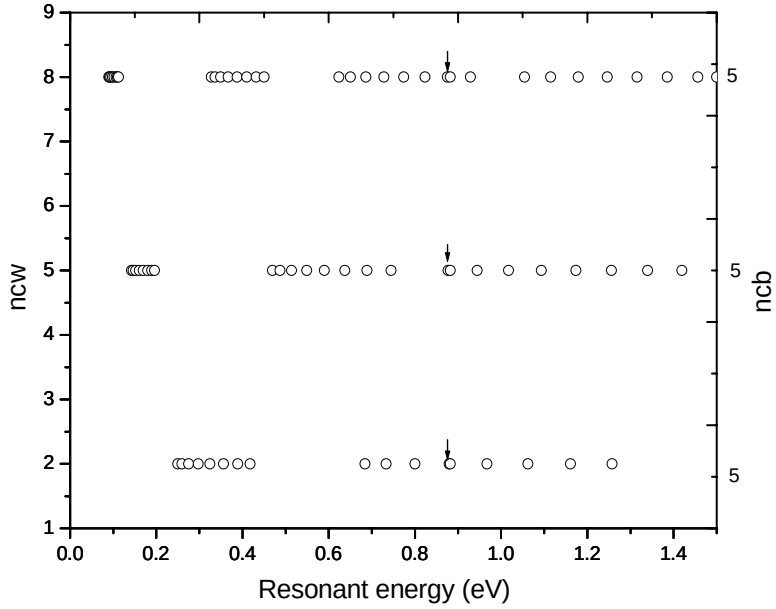

Figure 3(b)

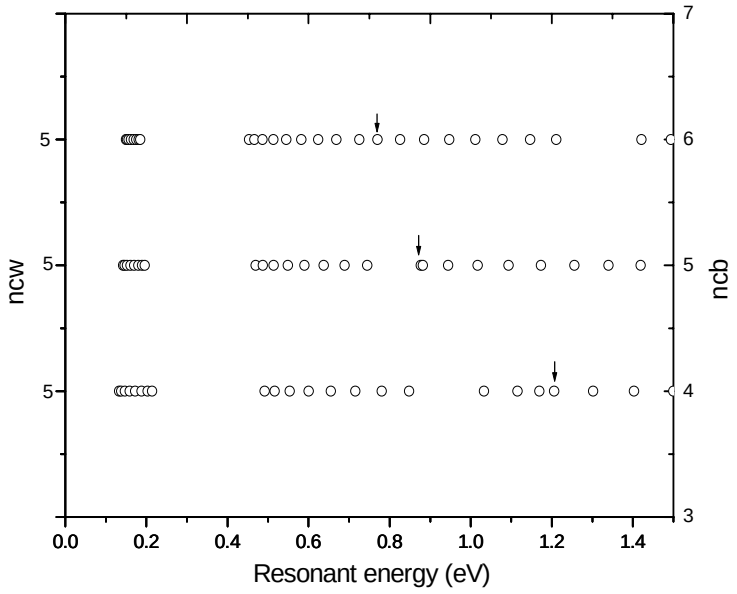

Figure 3(c)

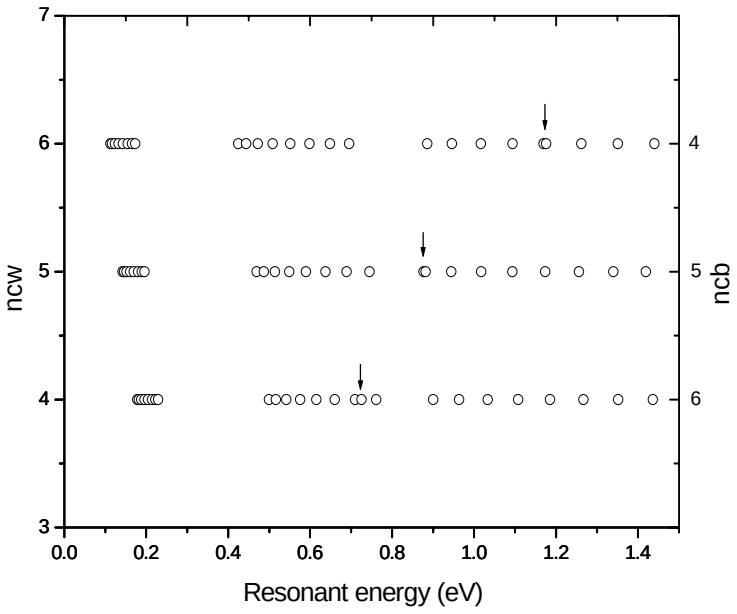

Figure 3(d)

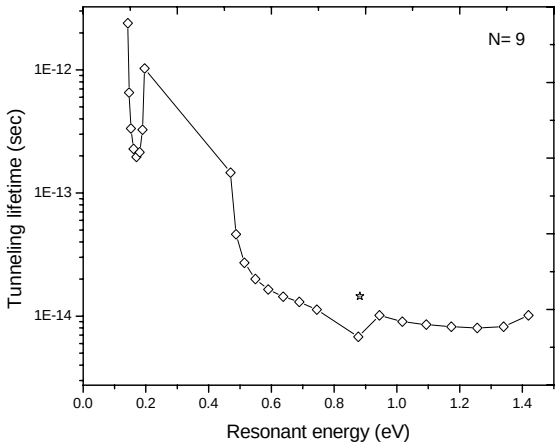

Figure 4(a)

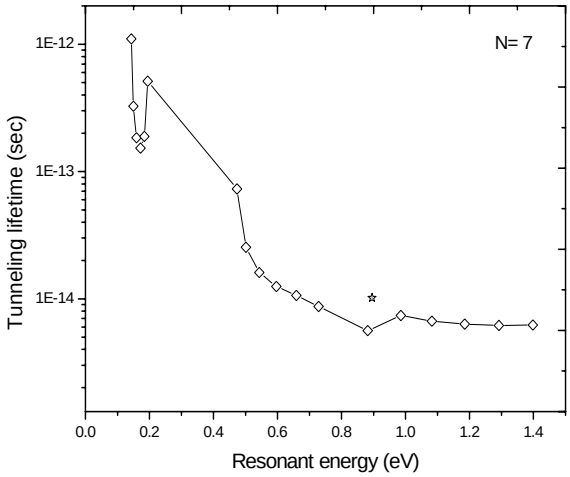

Figure 4(b)

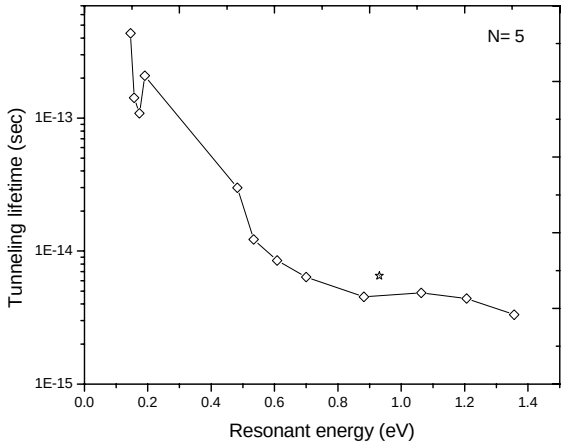

Figure 4 (c)

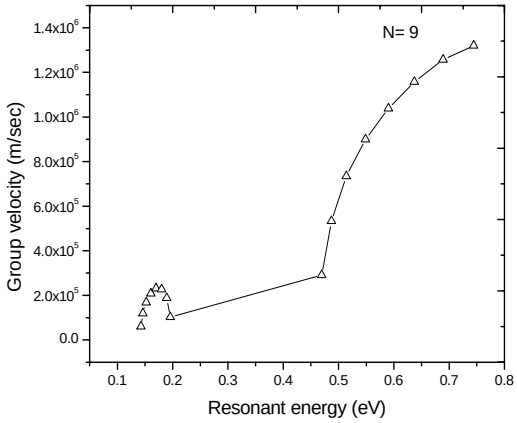

Figure 5(a)

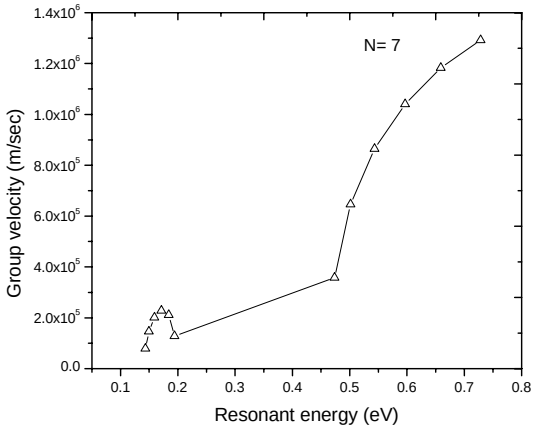

Figure 5(b)

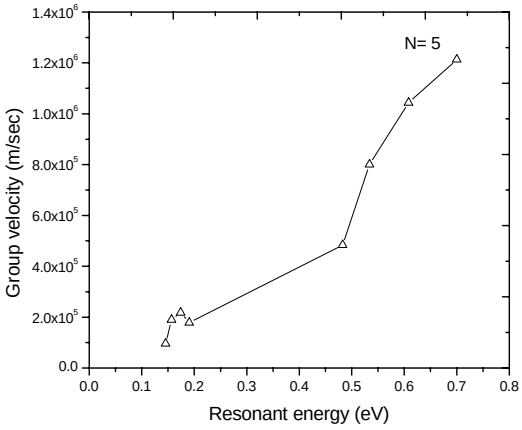

Figure 5(c)

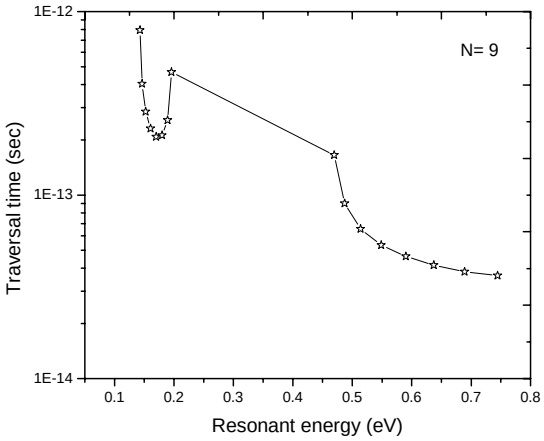

Figure 6(a)

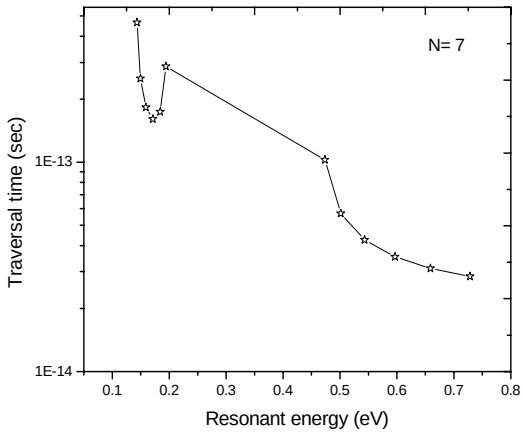

Figure 6(b)

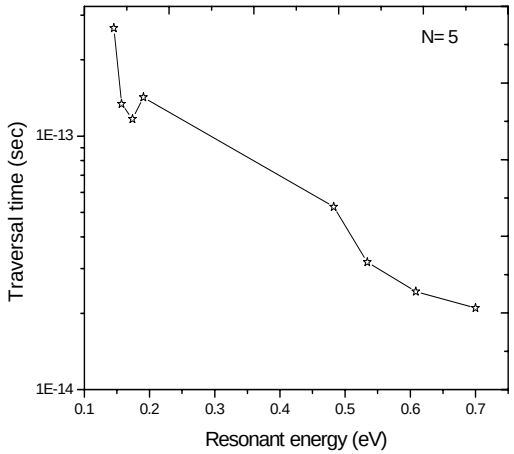

Figure 6(c)